

# Adaptive control of power receivers supply voltage in underground mines

Oleh Sinchuk <sup>1</sup>, Oleksii Mykhailenko <sup>1\*</sup>, Ihor Sinchuk <sup>1</sup>,  
Maryna Kotiakova <sup>1</sup>, Vladyslav Baranovskyi <sup>1</sup>, Mila Baranovska <sup>1</sup>

<sup>1</sup> Kryvyi Rih National University, Kryvyi Rih, Ukraine

\*Corresponding author: e-mail [mykhailenko@knu.edu.ua](mailto:mykhailenko@knu.edu.ua)

## Abstract

**Purpose.** This research aims to synthesize an automated system for stabilising the supply voltage of individual electrical consumers at iron ore mines when it deviates from standardised values due to unpredictable disturbances in the mine power systems.

**Methods.** A dynamic voltage restorer was used to stabilize the supply voltage of mine electrical consumers. The basic control system for the dynamic voltage restorer was developed using control theory methods, such as linear-quadratic control. Heuristic optimization methods were used to adapt the linear-quadratic regulator to unpredictable disturbances. The control integral absolute error was taken as the criterion. Numerical analysis was used to check the quality of transients during voltage stabilization using the proposed system.

**Findings.** The adaptive control system for a dynamic voltage restorer has been developed to stabilize the supply voltage of individual electrical consumers at iron ore mines. The optimal genetic algorithm parameters have been determined, including the population size and mutation rates of the linear-quadratic regulator weight matrices. It minimizes the integral absolute error and, as a result, eliminates overshoot (overshoot is no more than 0.058%) and reduces the transient time (up to 95%) compared to the unoptimized system.

**Originality.** The method of adaptive automated linear-quadratic regulator tuning based on a genetic algorithm is proposed. For the first time, it is used to control a dynamic voltage restorer installed between the power grid and the mine electrical consumer. This method has enabled the compensation of fluctuations in the mine power grid voltage at the consumer end, without overshoot and with short settling times.

**Practical implications.** The results can be used for the development of digital controllers embedded firmware for dynamic voltage restorers, providing real-time voltage fluctuation compensation and improving the power supply quality to mine electrical consumers.

**Keywords:** underground mine, power system, voltage control, dynamic voltage restorer, linear-quadratic regulation, genetic algorithm

## 1. Introduction

Within the set of power quality indicators (PQI) under the conditions of underground iron ore mining, two factors, among others, dominate: deviations of voltage and the range of its fluctuations from standardized values [1]-[3]. According to their ranking level [4], such voltage deviations and fluctuation ranges are caused by various factors, including pseudo-emergency situations (overloads) and actual emergencies (short circuits), variability and instability of power grid element parameters, unpredictable changes in electricity consumption levels of mine loads, as well as the consequences of attacks on energy facilities, among others [5]. Deviations of supply voltage from standardized (permissible) values negatively affect the operation of consumers connected to the industrial power grid, either on the surface or within the underground mine. To minimize these effects – or, ideally, to maintain PQI at standardized levels – in the practice of industrial

power supply systems (PSS), several approaches and corresponding technical measures are applied, including [5], [6]:

– adjustment of the transformation ratio of the power transformer at the corresponding substation;

– variation of the reactive power transmitted through transmission lines (TL), including adjustment of the electrical parameters of compensating devices (capacitor bank capacity, regulation of synchronous compensators).

At the same time, while noting the sufficiently broad “geography” of possible theories for implementing the aforementioned measures in the practice of power engineering complexes of underground mining enterprises, it is also appropriate to highlight the insufficient potential content of the current “portfolio” of such measures. This primarily concerns the lack of practical, application-oriented solutions in the development of technologies capable of ensuring an adequately natural response to the stochastic and rapidly changing factors influencing the process of maintaining real

PQI at standardized levels, both in local formats (individual indicators) and in the aggregate complex as a whole.

To address this gap, modern approaches, as substantiated in [7]-[13], propose the integration of a dynamic voltage restorer (DVR) into the constant maintenance of regulated PQI. Its function [13] is to compensate for voltage disturbances such as sags, swells, and harmonics. This ensures that consumers sensitive to voltage quality – whose share is significant within the power supply-consumption complex of underground mining enterprises – receive a stable and uninterrupted power supply.

At the same time, when implementing this provision, it should be understood that one of the key tasks in developing a DVR of this type for the power grids of underground iron ore enterprises is to ensure voltage stabilization within the internal power supply system of the enterprise under the influence of potentially unpredictable disturbing factors. Moreover, their impact on specific PQI may vary significantly. These prospects for DVR operation demonstrate that configuring a linear-quadratic regulator (LQR) solely by means of pole placement, for example, does not always allow for a full consideration of all dynamic properties of the system being controlled. This reduces the stability of automated control systems (ACS) and deteriorates the quality of transient processes (QTP).

It is generally recognized [14], [15] that for application in such automated control systems (ACS), the state-feedback approach – namely, the linear-quadratic regulator (LQR) method – is appropriate. This method belongs to the class of optimization-based regulator tuning techniques; therefore, its application to maintain a stable voltage level in underground power supply systems (PSS) under dynamic conditions is well justified. The LQR enables the achievement of the desired DVR state while simultaneously compensating for unpredictable disturbances by determining the necessary control actions.

In addition, the LQR minimizes a quadratic error criterion that includes terms for both state deviations and control efforts. This ensures the required accuracy of voltage (state) stabilization without abrupt changes, due to imposed constraints. By tuning the weighting matrices of the LQR, the desired response to unpredictable disturbances can be achieved without creating excessive loading on either the DVR filter, the inverter, or the individual electrical consumer. An analysis of power quality in the PSS of an actual underground iron ore mine has shown that DVR operation in such systems will require frequent, real-time maintenance of local PQI – namely, voltage deviations and the range of their fluctuations. If, at this time, the change in the control action is excessive, it will lead to reduced reliability of both the DVR equipment and the specific underground electricity consumer.

In addition to the above, it is worth noting that one of the advantages of the LQR in the context of DVR control is its ability to operate with state-space models involving multiple input and output variables. For the implementation of a DVR control system with coordinate transformations, the device model must include variables that describe the dynamics of DVR operation, such as the voltage across the capacitor of the LC filter and the load current, expressed in the d- and q-coordinate axes. This renders the model inherently multidimensional and thus suitable for the application of the LQR.

Additionally, the LQR enables adaptation to fluctuations in the power grid parameters or the DVR parameters by

continuously recalculating the quadratic error criterion with minimal computational complexity. This is particularly important since the PSS of underground mines are prone to unpredictable changes in load conditions or transmission line impedance. This feature also constitutes an advantage of the LQR over traditional ACS, which are not always capable of adapting to variable operating conditions due to the complexity of tuning or, in some cases, the complete absence of technical capability to perform such adjustments.

The selection of LQR weighting matrix values can also be performed using optimization methods based on criteria that ensure the desired transient performance indicators are met. In this way, the required DVR dynamics are achieved – overshoot, transient response time, or steady-state error are minimized. This enables the reduction of the DVR operation influence on transient processes in the underground mine power grid.

Thus, the application of the LQR method for DVR control under underground mine conditions is well justified. However, for the qualitative implementation of this method in practice, additional analysis is required to assess the impact of tuning levels on transient performance during real-time voltage stabilization.

At the same time, as demonstrated in [16], the variation of supply voltage for underground electrical consumers is nonlinear and stochastic in nature. This is primarily a result of the random character of disturbances acting within the mine power grid, a consequence of the stochastic behavior of electricity consumers. This feature becomes more pronounced at higher hierarchical levels of the power supply system, where the state directly depends on the aggregate operation of the enterprise electrical loads – their number and operating modes.

For the voltage quality indicators of local electrical consumers, the level of nonlinearity and stochasticity decreases. Within the range of operating modes that are close to or correspond to nominal values, the process can be linearized and considered as an almost deterministic case.

Under such conditions, controlling a DVR without a mechanism for adapting the control system parameters to random disturbances is practically impossible. Therefore, a necessary solution is to develop an adaptive control system for the dynamic voltage restorer to provide real-time regulation of the supply voltage for individual electrical consumers in the mine under the influence of disturbances present in the mine power supply system, as well as to assess the quality of the system dynamic characteristics during voltage stabilization under various operating conditions of specific electrical consumers. This will enhance the reliability and stability of the power distribution grid at mining enterprise.

The purpose of this research is to synthesize an adaptive control system for a dynamic voltage restorer with real-time regulation of its level, supplying individual electrical consumers of iron ore mines under actual conditions of voltage deviations from standardized values caused by unpredictable disturbances in the power supply system of the mine.

## 2. Methods

The selection of the state weighting matrix ( $W_x$ ) and the input weighting matrix ( $W_u$ ) for the LQR controller enables the achievement of transient performance (TP) that meets standardized requirements. However, determining appropriate values for these matrices is a challenge, as it requires a thorough understanding of the object dynamics and the con-

trol target to be achieved. Therefore, manual tuning is practically impossible or excessively complex, making it logical to automate this process.

In this context, the simplest option is an exhaustive search of all possible  $W_x$  and  $W_u$  values, but such an approach is highly time-consuming. An alternative is an analytical method, such as Bryson's rule [17], [18]. However, this method also provides only a "framework" estimation of  $W_x$  and  $W_u$ , and is, therefore, typically used only to determine initial values of the LQR matrices.

Thus, traditional methods of tuning the aforementioned parameters cannot guarantee sufficient transient performance. This is particularly true in complex systems, such as DVRs in underground mine PSS, where it is necessary to maintain a balance between several transient performance indicators – including overshoot, transient response time, and others – while simultaneously adapting to unpredictable disturbances.

Thus, when classical approaches cannot be applied due to various system-forming reasons, the use of population-based optimization methods appears appropriate, such as the genetic algorithm (GA), which is distinguished among them by its simplicity and efficiency [19], [20]. The GA employs evolutionary mechanisms, such as selection, crossover, and mutation, to determine the extremum of highly nonlinear response surfaces of the objective function (OF) by selecting chromosomes that minimize these OF values. This enables the identification of optimal LQR parameters for the DVR in the underground mine power grid, where the relationship between  $W_x$  and  $W_u$ , as well as transient performance (TP), is unknown and explicitly characterized as nonlinear.

When optimizing the parameters of an ACS with a multi-dimensional state-space model, such as a DVR, the response surface of the OF can be pretty complex. In such cases, many local minima may exist, which the GA avoids due to its stochastic mode of operation.

The GA is adapted to optimize  $W_x$  and  $W_u$  by defining an OF that quantitatively evaluates TP in the system. This OF may include key indicators such as overshoot, transient response time, and others. By encoding the values of  $W_x$  and  $W_u$  into chromosomes within a population, the GA generates diverse sets of encoded  $W_x$  and  $W_u$ , retaining and subsequently modifying those that provide the best compromise among various TP indicators, while discarding those that yield unsatisfactory results. Moreover, GAs are capable of solving multi-criteria optimization problems, ensuring that the process of identifying  $W_x$  and  $W_u$  accounts for the inherent trade-offs that inevitably arise in achieving standardized values of individual TP indicators.

However, implementing a GA is computationally expensive. The complexity of calculations increases with the growth of the population size and the number of generations. Nevertheless, the capabilities of parallel computing and the high clock frequencies of digital controllers have mitigated the impact of this problem. Furthermore, once sets of  $W_x$  and  $W_u$  values for the DVR LQR are obtained that are close to optimal, the ACS operates as a conventionally tuned LQR controller, without incurring additional computational costs for executing the GA during the real-time stabilization of the supply voltage for an underground electrical consumer.

Thus, the use of GA technology is a practical choice for optimizing  $W_x$  and  $W_u$  of the DVR LQR controller. This provides a foundation for obtaining more representative

dynamic characteristics of the ACS with a shorter LQR tuning time compared to conventional methods, such as exhaustive search or Bryson's rule, as well as other approaches.

Next, in the context of the search logic, consider a possible form of the OF for genetic optimization of the DVR LQR. Two approaches can be employed here. The first approach involves the direct determination of TP indicators and their aggregation into a single functional expression, as in [21]. The second approach utilizes a criterion that focuses on the deviation of the system output from the ACS reference, as in [22]. Such a criterion may be the integral absolute error (IAE).

The first approach, which involves the use of a generalized OF, requires extensive computations, thereby reducing its feasibility for real-time systems.

The second type of OF, namely the IAE criterion, minimizes the total error – the difference between the DVR output and the ACS reference (without separating steady-state and transient errors, or explicitly determining overshoot, transient response time, etc.). This method consistently and efficiently searches for the OF extremum and is proposed for application in this work.

### 3. Results and discussion

#### 3.1. Formulation of the control problem for a dynamic voltage restorer using a linear-quadratic regulator

The dynamic voltage restorer (DVR) (Fig. 1) comprises several key components that enable its operation in compensating voltage deviations from standardized values in the analysed electrical grid. In the circuit, an abstracted electrical consumer with motor M1 is protected from voltage deviations of varying magnitudes by the DVR device.

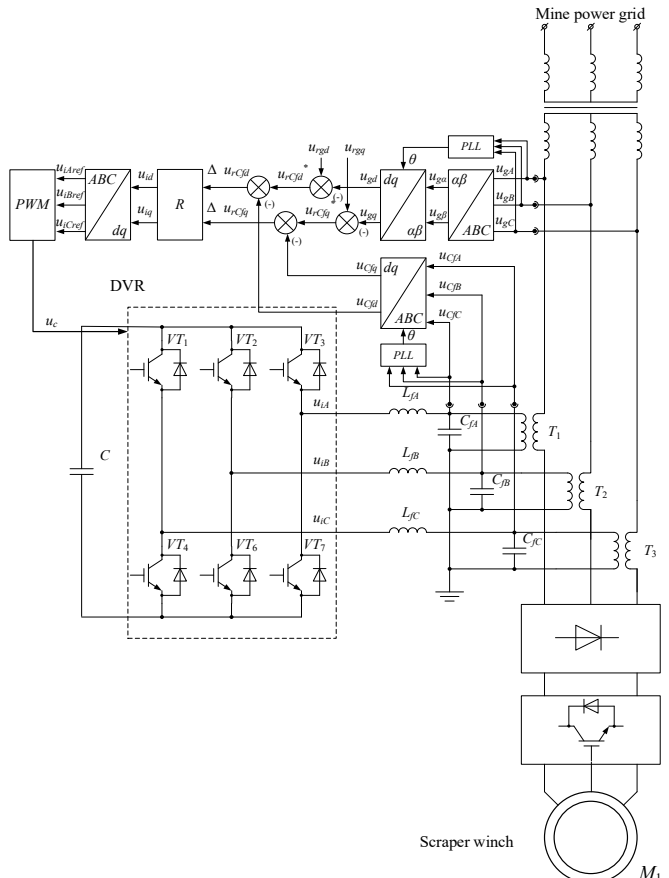


Figure 1. Functional control circuit of the dynamic voltage restorer

To compensate for voltage deviations, the DVR utilizes an energy storage system, which can comprise battery banks, supercapacitors, or similar devices. The stored energy is used to generate a compensating voltage that is added to the grid voltage, restoring it to its nominal level when it deviates from the standardized value. In the circuit, the storage element is represented by capacitor C.

The core of the DVR is a power converter, typically implemented based on a semiconductor inverter with pulse-width modulation (PWM). In the circuit (Fig. 1), the inverter is represented as a three-phase bridge with IGBT transistors VT1 through VT6. The device also includes matching transformers T1-T3, which provide galvanic isolation between the DVR and the grid, as well as voltage scaling, thereby increasing the level of the compensating voltage to the required value to maintain the desired supply voltage.

An essential element of the DVR is the filtering system, which eliminates high-frequency components generated during inverter operation, preventing their propagation into the grid. Typically, it is implemented using passive filters. Figure 1 illustrates the most common filter configuration, specifically a three-phase LC filter comprising elements  $L_{fA}C_{fA}$ ,  $L_{fB}C_{fB}$ , and  $L_{fC}C_{fC}$ . The cutoff frequency of the filter is selected during the DVR design stage, depending on the topology of the semiconductor voltage-source inverter.

The operation of the DVR is coordinated by the ACS, which includes measuring instruments for real-time monitoring of grid voltage parameters, as well as a regulator that, according to a specified algorithm, controls the IGBT transistors of the inverter to generate the appropriate compensating voltage waveform added to the grid voltage.

Figure 1 shows the basic control circuit of the DVR based on coordinate converters, which operates as follows. The measured three-phase grid voltage  $u_{gA}$ ,  $u_{gB}$ ,  $u_{gC}$  is transformed into a two-phase system  $u_{ga}$ ,  $u_{gb}$  and then into a two-phase system  $u_{gd}$ ,  $u_{gq}$  by applying the Park transformation. To determine the rotation angle of the system  $dq$ , a phase-locked loop (PLL) is employed. Next, summators determine the difference between the current grid voltage  $u_{gd}$ ,  $u_{gq}$  and the reference normalized values  $u_{rgd}$ ,  $u_{rgq}$ . The resulting values  $u_{rcfd}^*$  and  $u_{rcfq}^*$  serve as reference signals for the ACS of the inverter. The  $u_{rcfd}^*$  and  $u_{rcfq}^*$  are then compared with the values of the voltage transformed into the system  $dq$ , denoted as  $u_{CfA}$ ,  $u_{CfB}$ , and  $u_{CfC}$ , which are measured across the capacitors of the LC filter, i.e.,  $u_{Cfd}$ ,  $u_{Cfq}$ . These voltages represent the controlled variable of the system. The difference between the reference and the measured filter voltages is fed to the regulator (R). The control algorithm of the regulator may vary, ranging from a classical PI or PID controller to a fuzzy logic controller. The regulator then generates reference values  $u_{ia}$ ,  $u_{ib} \rightarrow u_{iAref}$ ,  $u_{iBref}$ ,  $u_{iCref}$  for the pulse-width modulator (PWM), which controls the IGBT transistors of the inverter.

The DVR model can be represented in the state-space form [23], [24]:

$$\begin{cases} x' = Ax + Bu + B_d d; \\ y = Cx + Du + D_d d, \end{cases} \quad (1)$$

where:

$$A = \begin{bmatrix} -\frac{R_\phi}{L_\phi} & \omega & -\frac{1}{L_\phi} & 0 \\ -\omega & -\frac{R_\phi}{L_\phi} & 0 & -\frac{1}{L_\phi} \\ \frac{1}{C_\phi} & 0 & 0 & \omega \\ 0 & \frac{1}{C_\phi} & -\omega & 0 \end{bmatrix}, B = \begin{bmatrix} \frac{1}{L_\phi} & 0 \\ 0 & \frac{1}{L_\phi} \\ 0 & 0 \\ 0 & 0 \end{bmatrix}, \quad (2)$$

$$B_d = \begin{bmatrix} 0 & 0 & -\frac{1}{C_\phi} & 0 \\ 0 & 0 & 0 & -\frac{1}{C_\phi} \end{bmatrix}, C = \begin{bmatrix} 0 & 0 & 1 & 0 \\ 0 & 0 & 0 & 1 \end{bmatrix}.$$

The state-space model of the DVR is characterized by the following parameters:  $C_f = 47 \mu F$ ,  $L_f = 0.5 mH$ ,  $R_f = 1 \Omega$ . They are determined under the assumption that individual voltage stabilization is applied for a typical electrical consumer in an underground mine – specifically, a scraper winch of the LS-30 type (rated power – 30 kW).

To achieve high-quality TP of the DVR as a dynamic system (1)-(2), such as minimal overshoot and reduced transient response time, it is necessary to implement the following form of control:

$$u = -Kx. \quad (3)$$

The ACS scheme of the DVR with state-feedback LQR is presented in Figure 2. In the diagram, the object – the state-space model – is marked in yellow, while the control block is marked in red. The LQR, using specific weighting matrices

$W_x$  and  $W_u$ , together with the state data  $\begin{bmatrix} u_{Cfd} \\ u_{Cfq} \\ i_{Lfd} \\ i_{Lfq} \end{bmatrix}$ , the input  $\begin{bmatrix} r_{u_{Cfd}} \\ r_{u_{Cfq}} \end{bmatrix}$ , the disturbance  $\begin{bmatrix} i_{Ld} \\ i_{Lq} \end{bmatrix}$ , and the output  $\begin{bmatrix} u_{Cfd} \\ u_{Cfq} \end{bmatrix}$ , determines the optimal feedback matrix  $K$ .

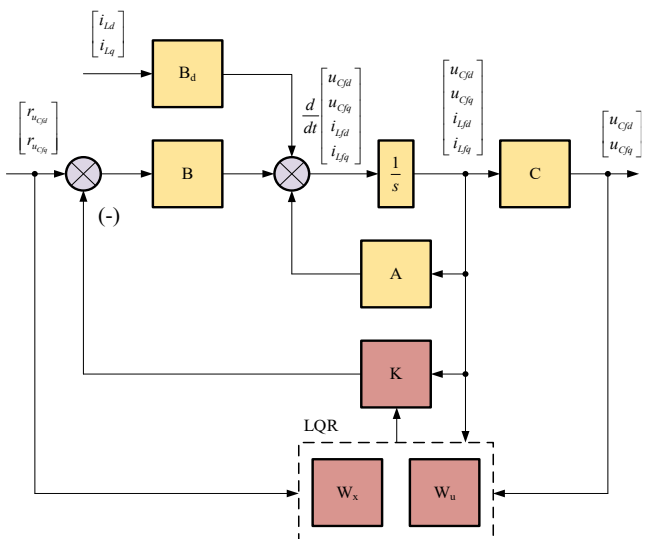


Figure 2. Block diagram of a dynamic voltage restorer control system with a linear-quadratic regulator

In such an ACS with an LQR, obtaining the desired control requires minimization of the following functional:

$$J = \int_0^{\infty} [x^T(t)W_x x(t) + u^T(t)W_u u(t)] dt, \quad (4)$$

where:

$W_x$  – the state variable weighting matrix is symmetric and positive semi-definite,  $k \times k$ ;

$W_u$  – the control weighting matrix is symmetric and positive definite,  $n \times n$ .

To solve the optimization problem, the Hamiltonian function is defined as:

$$H = x^T W_x x + u^T W_u u + \lambda (Ax + Bu), \quad (5)$$

where:

$\lambda(t)$  – Lagrange multiplier.

The necessary conditions for obtaining the optimal solution are as follows:

The equation with the Lagrange multiplier is:

$$\dot{\lambda}(t) = -\frac{\partial H}{\partial x} = -Qx - A^T \lambda. \quad (6)$$

The equation of optimal control is:

$$\frac{\partial H}{\partial u} = 2W_u u + B^T \lambda = 0. \quad (7)$$

From which:

$$u = -\frac{1}{2}W_u^{-1}B^T \lambda. \quad (8)$$

The solution is then obtained by solving the Algebraic Riccati Equation (ARE).

Assume that the optimization functional has a quadratic form:

$$V(x) = x^T S x, \quad (9)$$

where:

$S$  – symmetric positive definite matrix.

Lagrange multiplier:

$$\lambda = \frac{\partial V}{\partial x} = 2Sx. \quad (10)$$

Substituting into (3):

$$u = -W_u^{-1}B^T S x. \quad (11)$$

The equation of the closed-loop system takes the form:

$$\frac{dx}{dt} = (A - BW_u^{-1}B^T S)x. \quad (12)$$

Substituting into Equation (10):

$$2S(A - BW_u^{-1}B^T S)x = -Qx - A^T(2Sx). \quad (13)$$

Eliminating  $x$ :

$$SA + A^T S - SBW_u^{-1}B^T S + Q = 0. \quad (14)$$

By interchanging the first and second terms, we obtain the ARE:

$$A^T S + SA - SBW_u^{-1}B^T S + Q = 0. \quad (15)$$

The solution of the ARE (15) yields the matrix  $S$ , through which the optimal state-feedback gain matrix is determined:

$$K = W_x^{-1}B^T S, \quad (16)$$

which gives the optimal control law:

$$u = -Kx = W_x^{-1}B^T S x. \quad (17)$$

Randomly assign values to the state variable weighting matrix and the control weighting matrix:

$$W_x = \begin{bmatrix} 400 & 0 & 0 & 0 \\ 0 & 400 & 0 & 0 \\ 0 & 0 & 10 & 0 \\ 0 & 0 & 0 & 10 \end{bmatrix}; W_u = \begin{bmatrix} 15 & 0 \\ 0 & 15 \end{bmatrix}. \quad (18)$$

The solution to the ARE is (15):

$$S = \begin{bmatrix} 0.036141 & 0 & 0.002183 & 0 \\ 0 & 0.036141 & 0 & 0.002183 \\ 0.002183 & 0 & 0.004591 & 0 \\ 0 & 0.002183 & 0 & 0.004591 \end{bmatrix}. \quad (19)$$

Poles:

$$p = \begin{bmatrix} (-5.818766 + 4.905226j) \cdot 10^3 \\ (-5.818766 - 4.905226j) \cdot 10^3 \\ (-5.818766 + 4.2769077j) \cdot 10^3 \\ (-5.818766 - 4.2769077j) \cdot 10^3 \end{bmatrix}. \quad (20)$$

State-feedback gain matrix:

$$K = \begin{bmatrix} 4.81877 & 0 & 0.290994 & 0 \\ 0 & 4.81877 & 0 & 2.290994 \end{bmatrix}. \quad (21)$$

Table 1 and Figure 3 present the numerical characteristics of the transient performance indicators and the transient response itself in the closed-loop system.

**Table 1. Performance of the closed-loop system of the dynamic voltage restorer with matrices (18)**

Transient characteristics	Time, s	Overshoot, %	Time, s	Overshoot, %
Input / Output	$u_{Cfd}$		$u_{Cfq}$	
$u_{id}$	0.00049	1.795	0.001	7.789
$u_{iq}$	0.001	7.789	0.00049	1.795
$i_{Ld}$	0.00066	2.695	0.00093	16.35
$i_{Lq}$	0.00093	16.35	0.00066	2.695

As the obtained results indicate, the DVR system exhibits overshoot, and the transient response time is pretty significant. Then, perform the tuning of the LQR by determining the optimal values of the weighting matrices using a genetic algorithm. Subsequently, the synthesis of the adaptive control algorithm is carried out.

### 3.2. Development of an adaptive control algorithm for the dynamic voltage restorer

Figure 4 illustrates the simplified structure of the DVR ACS, which utilizes the LQR tuned by the GA, the adaptive control algorithm developed for this purpose. The blocks used for the evolutionary optimization of the LQR are marked in green: the “Objective Function” block, which computes the OF value, and the “GA” block, which implements the algorithm for minimizing the OF. The data transmission channels used to determine the control actions of the regulator (17), as shown in Figure 2, are not depicted in this diagram. During optimization, the GA selects chromosomes with lower IAE values. This creates a high probability that subsequent generations will yield  $W_x$  and  $W_u$  for the LQR with improved accuracy.

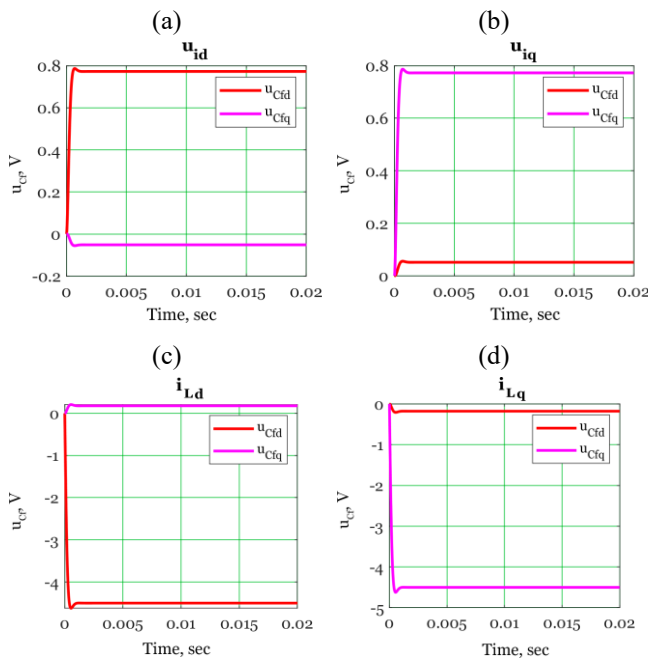


**Figure 3. Transient response in the closed-loop system with a linear-quadratic regulator using matrices (18) under a unit step function: (a) channel “inverter voltage  $d$  – filter capacitor voltage”; (b) channel “inverter voltage  $q$  – filter capacitor voltage”; (c) channel “load current  $d$  – filter capacitor voltage”; (d) channel “load current  $q$  – filter capacitor voltage”**

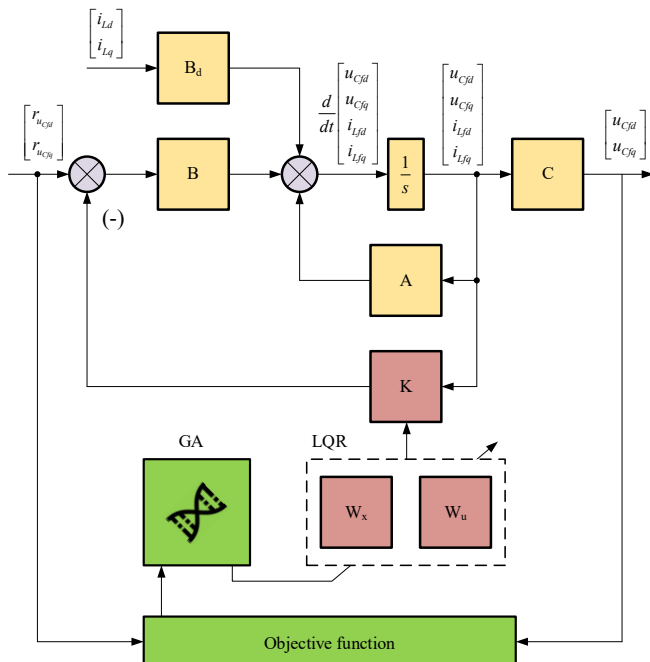
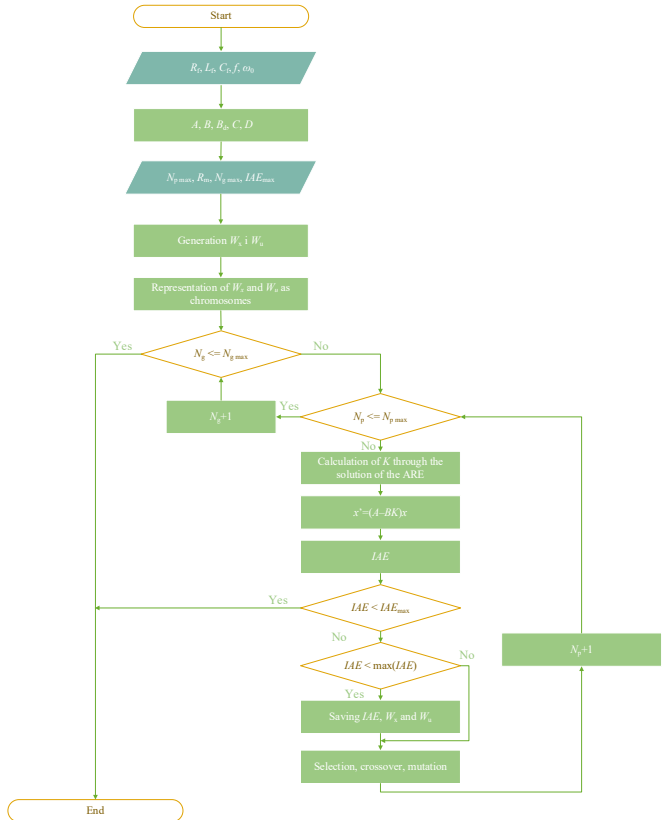


Figure 4. Block diagram of a dynamic voltage restorer control system with a linear-quadratic regulator tuned by a genetic algorithm

Figure 5. Block diagram of the DVR control algorithm with an LQR tuned by a GA. In the first step, the parameters of the equivalent circuit of the DVR are defined: active resistance  $R_f$ , inductance  $L_f$ , capacitance  $C_f$ , frequency  $f$ , and angular frequency  $\omega_0 = 2\pi f$ . These parameters determine the electrical properties of the system for real-time voltage stabilization of the mine electrical consumer. Based on them, the mathematical model of the DVR is constructed.



**Figure 5. Control algorithm of the dynamic voltage restorer with a linear-quadratic regulator tuned by a genetic algorithm**

Next, the state-space model of the DVR is initialized, represented by the matrices  $A$ ,  $B$ ,  $B_d$ ,  $C$ , and  $D$ .

In the next step, the parameters of the genetic algorithm used to optimize the weighting matrices of the LQR are defined: population size ( $N_p$ ) – specifies the number of possible solutions in each generation; mutation rate ( $R_m$ ) – determines the intensity of changes in the selected chromosomes; and number of generations ( $N_g$ ) – defines how many cycles the algorithm will execute before termination.

The boundary value of the IAE ( $IAE_{max}$ ) is also defined:

$$J = \max \left( \int_0^T |e_i(t)| dt, \int_0^T |e_{i+1}(t)| dt, \dots, \int_0^T |e_{i+N}(t)| dt \right), \quad (22)$$

where:

$e_i = r_i - y_i$  – the difference between the DVR output and the LQR controller reference;

$T$  – control duration.

After that, the initial population of weighting matrices  $W_x$  and  $W_u$  for the DVR LQR controller is generated within the defined boundaries.  $W_x$  and  $W_u$  are filled with random values. This enables the identification of various starting points within the OF landscape, thereby accelerating the optimization of the LQR. Next, each set of  $W_x$  and  $W_u$  in the population is encoded as chromosomes containing the values of all diagonal elements of the LQR weighting matrices. This is required for the operation of the GA, since selection, crossover, and mutation are applied only to chromosomes.

At this point, the main loop of the algorithm begins. Initially, for each set of  $W_x$  and  $W_u$ , the feedback gain matrix  $K$  is computed by solving the ARE. After that, the closed-loop DVR system is simulated, where the control actions are determined using the obtained matrix  $K$ , allowing for the

evaluation of DVR behavior when applying the LQR with the identified  $W_x$  and  $W_u$ .

Following the simulation, the IAE is calculated, which quantitatively assesses the quality of the obtained solution.

The obtained IAE value is compared with the boundary IAE. If the solution satisfies the condition, the GA terminates, and the current values of  $W_x$  and  $W_u$  are considered optimal. Otherwise, the optimization continues.

If the IAE is smaller than that obtained in previous cycles of the algorithm, the current IAE and the corresponding LQR weighting matrices  $W_x$  and  $W_u$  are retained. The population then evolves: the GA selects the best solutions for the LQR. Chromosomes with lower IAE values have a higher probability of crossover.

Subsequently, crossover is performed: two parent chromosomes, each encoding a set of LQR matrices, exchange segments, thereby generating new solutions. Various crossover techniques can be employed to ensure high-quality recombination of the parent chromosomes.

The final step in the GA cycle is mutation. A random alteration of chromosome elements is performed, preserving the diversity of the LQR weighting matrix population and preventing the GA from prematurely terminating in a local minimum of the OF.

The GA cycle is repeated until either the maximum number of generations is reached or the optimal values of  $W_x$  and  $W_u$  for the DVR LQR are found, ensuring the minimum IAE.

The DVR LQR controller is optimized using the algorithm shown in Figure 5. For configuring the GA, set the number of chromosomes to  $N_p = 40$ , the probabilities of crossover and mutation to 80%, and the number of chromosomes transferred to the next generation without crossover and mutation to 20%. Since  $W_x$  and  $W_u$  consist of real numbers, it is appropriate to apply an arithmetic crossover method of the following form:

$$O = \psi P_1 + (1-\psi) P_2, \quad (23)$$

where  $O$  – offspring chromosome;

$P_1, P_2$  – parent chromosomes;

$\psi$  – crossover coefficient of the parent chromosomes.

### 3.3. Simulation of the closed-loop control system of the dynamic voltage restorer using a genetic algorithm

Based on [25]-[27], the mutation rate has a decisive influence on the speed of OF minimization when applying the GA. Therefore, consider several variations of mutation rate values for the  $W_x$  ( $R_{mWx}$ ) matrix and the  $W_u$  ( $R_{mWu}$ ) matrix. Initially, they are set to the following values:  $R_{mWx} = 4$  and  $R_{mWu} = 1$ .

As the termination condition of the GA, we define the completion of a specified number of evolutionary generations. For the simulation, assume  $N_g = 200$ .

After running the GA with optimization according to criterion (22),  $W_x$  and  $W_u$  were determined:

$$W_x = \begin{bmatrix} 226.73 & 0 & 0 & 0 \\ 0 & 44.046 & 0 & 0 \\ 0 & 0 & 332.49 & 0 \\ 0 & 0 & 0 & 246.66 \end{bmatrix}; \quad (24)$$

$$W_u = \begin{bmatrix} 0.1 & 0 \\ 0 & 0.1 \end{bmatrix}.$$

The state-feedback matrix, obtained from the solution of the ARE in accordance with the LQR weighting matrices  $W_x$  and  $W_u$  (24):

$$K_{opt} = \begin{bmatrix} 57.94017 & 0.07846 & 56.6665 & 0.17039 \\ 0.078459 & 37.43409 & 0.24499 & 48.67799 \end{bmatrix}. \quad (25)$$

Figure 6 illustrates the process of evolutionary search for the optimal  $W_x$  and  $W_u$  of the DVR LQR.

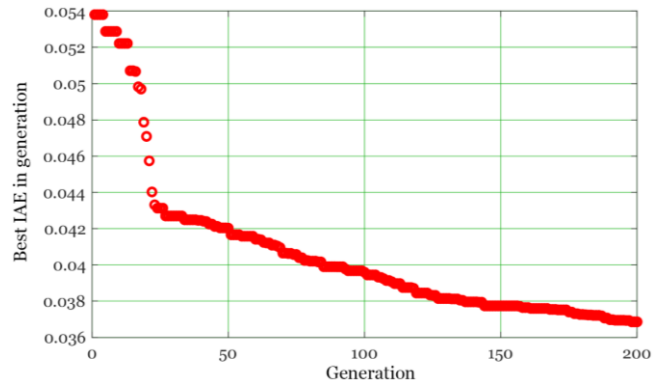


**Figure 6. Variation of the integral absolute error during evolutionary optimization of the linear-quadratic regulator (genetic algorithm parameters  $R_{mWx} = 4$  and  $R_{mWu} = 1$ )**

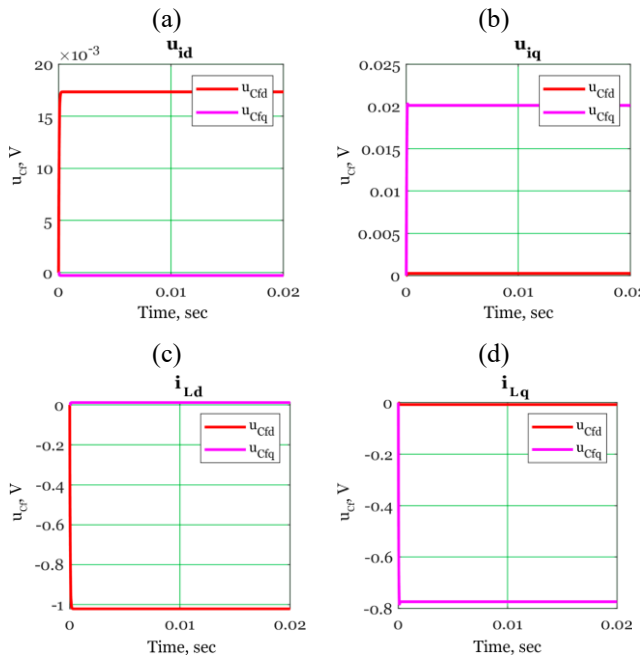
As can be observed, the minimization is initially quite intensive, but after approximately the 25<sup>th</sup> generation, it proceeds more smoothly. According to the graph, after 200 generations, the optimal values of  $W_x$  and  $W_u$  were not yet determined, and the search would continue.

Table 2 and Figure 7 present the numerical characteristics of the transient performance indicators and the transient response in the closed-loop system with the LQR using the values of  $W_x$  and  $W_u$  obtained at the 200<sup>th</sup> generation of the GA.

**Table 2. Performance of the optimized linear-quadratic regulator of dynamic voltage restorer (genetic algorithm parameters  $R_{mWx} = 4$  and  $R_{mWu} = 1$ )**

Transient characteristics	Time, s	Overshoot, %		Time, s	Overshoot, %
		$u_{Cfd}$	$u_{Cfq}$		
$u_{id}$	$0.1598 \cdot 10^{-3}$	0	$0.2231 \cdot 10^{-3}$	3.6973	
$u_{iq}$	$0.1611 \cdot 10^{-3}$	1.2723	$0.2091 \cdot 10^{-3}$	3.2766	
$i_{Ld}$	$0.1502 \cdot 10^{-3}$	0	$0.2174 \cdot 10^{-3}$	4.1863	
$i_{Lq}$	$0.2148 \cdot 10^{-3}$	3.6917	$0.1878 \cdot 10^{-3}$	4.995	

Considering transient response time as a TP indicator, the LQR optimized by the GA demonstrates a significant acceleration in the transition between steady states compared with the non-tuned system. The most significant reduction in transient response time was observed for channel  $u_{iq} - u_{Cfd}$ , by 97%, while the most minor reduction – 93.19% was recorded for channel  $u_{iq} - u_{Cfq}$ . When compared with the indicators of the closed-loop DVR system with the LQR, where  $W_x$  and  $W_u$  were assigned randomly (Table 1), a reduction in transient response time is also observed. Once again, the most significant and minor accelerations of the transient response occurred for the channels linking the DVR inverter voltage with the voltage across the LC filter capacitor, namely  $u_{iq} - u_{Cfd}$  and  $u_{iq} - u_{Cfq}$  – for which the reductions in transient response time amounted to 83.89% and 57.33%, respectively. For the other channels, the transient response time decreased by 76-77%.



**Figure 7. Transients in the closed-loop system with optimized linear-quadratic regulator (genetic algorithm parameters  $R_{mWx} = 4$  and  $R_{mWu} = 1$ ): (a) channel “inverter voltage  $d$  – filter capacitor voltage”; (b) channel “inverter voltage  $q$  – filter capacitor voltage”; (c) channel “load current  $d$  – filter capacitor voltage”; (d) channel “load current  $q$  – filter capacitor voltage”**

As can be seen from Table 2, overshoot is completely absent for channels  $u_{id} - u_{Cfd}$  and  $i_{Ld} - u_{Cfd}$ , and where it does occur, its value does not exceed the standardized limit of 5%. When compared with the indicators of the closed-loop DVR system with randomly tuned weighting matrices of the LQR (Table 1), a reduction in overshoot was also observed in the system with the GA-optimized LQR for channels other than  $u_{iq} - u_{Cfq}$  and  $i_{Lq} - u_{Cfd}$ . Specifically, for  $u_{id} - u_{Cfq}$ , the reduction amounted to 52.53%, for  $u_{iq} - u_{Cfd}$  – 83.67%, for  $i_{Ld} - u_{Cfq}$  – 74.39%, and for  $i_{Lq} - u_{Cfd}$  – 77.42%. Of course, channels without regulation, such as  $u_{id} - u_{Cfd}$  and  $i_{Ld} - u_{Cfd}$  are not mentioned here. For the aforementioned  $u_{iq} - u_{Cfq}$  and  $i_{Lq} - u_{Cfd}$ , no reduction occurred. Overshoot for  $u_{iq} - u_{Cfq}$  in the non-optimized GA control system was 3.2766% compared to 1.795% in the optimized one, while for  $i_{Lq} - u_{Cfd}$  it was 4.995% versus 2.695%, respectively.

Thus, overall, the optimization of the weighting matrices using the GA has a positive effect on the operation of the closed-loop ACS with the LQR. Then, perform simulations with slightly different GA parameters and compare the obtained results.

Reduce the mutation rates of the LQR weighting matrices by half, specifically to the values  $R_{mWx} = 2$  and  $R_{mWu} = 0.5$ .

Weighting matrices of state variables and control actions:

$$W_x = \begin{bmatrix} 127.75 & 0 & 0 & 0 \\ 0 & 258.62 & 0 & 0 \\ 0 & 0 & 392.27 & 0 \\ 0 & 0 & 0 & 459.42 \end{bmatrix}; \quad (26)$$

$$W_u = \begin{bmatrix} 0.1122 & 0 \\ 0 & 0.1 \end{bmatrix}.$$

Optimized state-feedback matrix:

$$K_{opt} = \begin{bmatrix} 49.86778 & -0.04052 & 62.31003 & -0.13744 \\ -0.04052 & 37.43409 & -0.11372 & 66.7858 \end{bmatrix}. \quad (27)$$

Figure 8 shows that in this case also, after 200 generations, the optimal values of  $W_x$  and  $W_u$  were not determined, and the evolutionary search for the DVR LQR tuning would continue.

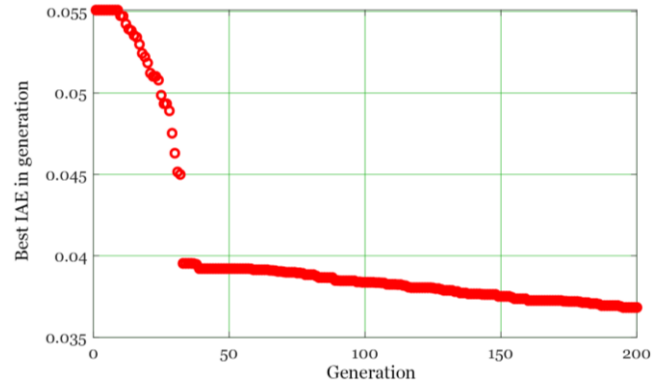


**Figure 8. Variation of the integral absolute error during evolutionary optimization of the linear-quadratic regulator (genetic algorithm parameters  $R_{mWx} = 2$  and  $R_{mWu} = 0.5$ ): first model run**

Analyzing the data from Table 3 regarding transient response time, it can be stated that acceleration occurs when compared with the results of the closed-loop system with both the non-optimized LQR controller (Table 1) and the optimized LQR controller (Table 2).

**Table 3. Performance of the optimized linear-quadratic regulator of dynamic voltage restorer (genetic algorithm parameters  $R_{mWx} = 2$  and  $R_{mWu} = 0.5$ ): first model run**

Transient characteristics	Time, s	Overshoot, %		Overshoot, %
		$u_{Cfd}$	$u_{Cfq}$	
Input / Output		$u_{Cfd}$	$u_{Cfq}$	
$u_{id}$	$0.1148 \cdot 10^{-3}$	0.3689	$0.1595 \cdot 10^{-3}$	0.0853
$u_{iq}$	$0.1494 \cdot 10^{-3}$	0.2184	$0.1458 \cdot 10^{-3}$	0
$i_{Ld}$	$0.092 \cdot 10^{-3}$	0.5259	$0.1369 \cdot 10^{-3}$	0.2482
$i_{Lq}$	$0.1375 \cdot 10^{-3}$	0.2748	$0.1291 \cdot 10^{-3}$	0

We compare only with the latter case, as it demonstrated the lowest transient response time across all channels among the three systems considered. The most significant reduction in transient response time was 38.74 and 37.03% for channels  $i_{Ld} - u_{Cfd}$  and  $i_{Lq} - u_{Cfq}$ , respectively.

The most minor reduction was 7.26% for channel  $u_{iq} - u_{Cfd}$ , for channels  $u_{id} - u_{Cfd}$ ,  $u_{id} - u_{Cfq}$ ,  $u_{iq} - u_{Cfq}$ ,  $i_{Lq} - u_{Cfd}$  and  $i_{Ld} - u_{Cfq}$  the reduction in transient response time amounted to 28.16, 28.5, 30.27, 35.96, and 31.26%, respectively. Thus, the duration of the transition between steady-state values is very short (Fig. 9).

Analyzing the data on overshoot (Table 2), it can be seen that for channels  $u_{iq} - u_{Cfq}$  and  $i_{Lq} - u_{Cfq}$  it is absent. In all other channels, according to the state-space model of the DVR, this indicator does not exceed 1%, representing the optimal ACS configuration among all those obtained. Comparing the results with the non-optimized system (Table 1), in the GA-optimized system, a slight overshoot appeared in channels  $u_{id} - u_{Cfd}$  and  $i_{Ld} - u_{Cfd}$ , while for channels  $u_{id} - u_{Cfq}$ ,  $u_{iq} - u_{Cfd}$ ,  $i_{Ld} - u_{Cfq}$  and  $i_{Lq} - u_{Cfd}$  it was reduced by 97.69, 82.83, 94.07, and 92.56%, respectively.

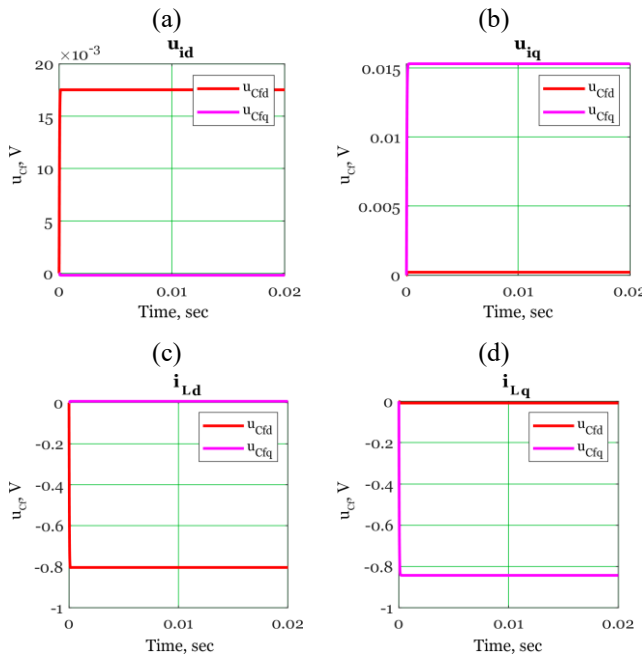


**Figure 9.** Transients in the closed-loop system with optimized linear-quadratic regulator (genetic algorithm parameters  $R_{mW_x} = 2$  and  $R_{mW_u} = 0.5$ ) during first model run: (a) channel “inverter voltage  $d$  – filter capacitor voltage”; (b) channel “inverter voltage  $q$  – filter capacitor voltage”; (c) channel “load current  $d$  – filter capacitor voltage”; (d) channel “load current  $q$  – filter capacitor voltage”

Perform another simulation of the evolutionary search for the optimal values of  $W_x$  and  $W_u$  of the DVR LQR with GA settings  $R_{mW_x} = 2$  and  $R_{mW_u} = 0.5$ .

Weighting matrices of state variables and control actions:

$$W_x = \begin{bmatrix} 192.97 & 0 & 0 & 0 \\ 0 & 212.1096 & 0 & 0 \\ 0 & 0 & 377.28 & 0 \\ 0 & 0 & 0 & 405.03 \end{bmatrix}; \quad (28)$$

$$W_u = \begin{bmatrix} 0.1 & 0 \\ 0 & 0.1 \end{bmatrix}.$$

Optimized state-feedback matrix:

$$K_{opt} = \begin{bmatrix} 55.71405 & -0.00841 & 60.4317 & -0.030759 \\ -0.00841 & 57.7798 & -0.02999 & 62.64937 \end{bmatrix}. \quad (29)$$

Examining the graph (Fig. 10), it is evident that the evolutionary search for the values of  $W_x$  and  $W_u$  proceeds quite intensively. Still, after approximately the 60<sup>th</sup> generation, it begins to progress more smoothly. From the 140<sup>th</sup> generation onward, the IAE value practically no longer changes, meaning that optimal DVR LQR settings were found before reaching the maximum number of generations in this simulation.

Table 4 and Figure 11 present the numerical characteristics of the transient performance indicators and the transient response in the closed-loop system.

The data from Table 4 show that in this simulation, the transient response time increased compared to the previous case (Table 3). Still, it remains relatively low when compared to the non-optimized GA closed-loop system. Such an LQR controller can be applied in the control of the DVR.

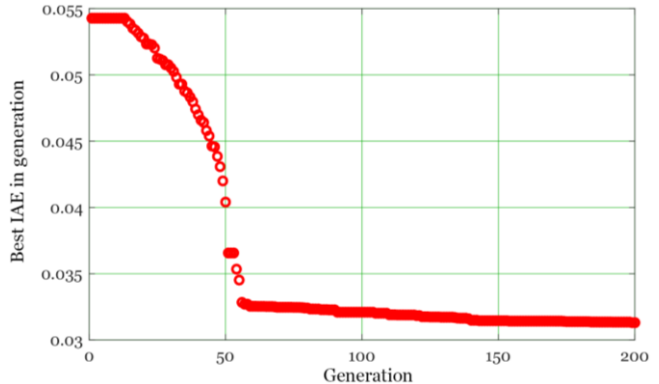


**Figure 10.** Variation of the integral absolute error during evolutionary optimization of the linear-quadratic regulator (genetic algorithm parameters  $R_{mW_x} = 2$  and  $R_{mW_u} = 0.5$ ): second model run

**Table 4.** Performance of the optimized linear-quadratic regulator of dynamic voltage restorer (genetic algorithm parameters  $R_{mW_x} = 2$  and  $R_{mW_u} = 0.5$ ): second model run

Transient characteristics	Time, s	Overshoot, %	Time, s	Overshoot, %
Input / Output	$u_{Cfd}$			
$u_{id}$	$0.1386 \cdot 10^{-3}$	0	$0.1735 \cdot 10^{-3}$	0
$u_{iq}$	$0.1824 \cdot 10^{-3}$	0	$0.1395 \cdot 10^{-3}$	0.0058
$i_{Ld}$	$0.1283 \cdot 10^{-3}$	0	$0.169 \cdot 10^{-3}$	0
$i_{Lq}$	$0.1711 \cdot 10^{-3}$	0	$0.1205 \cdot 10^{-3}$	0.0008

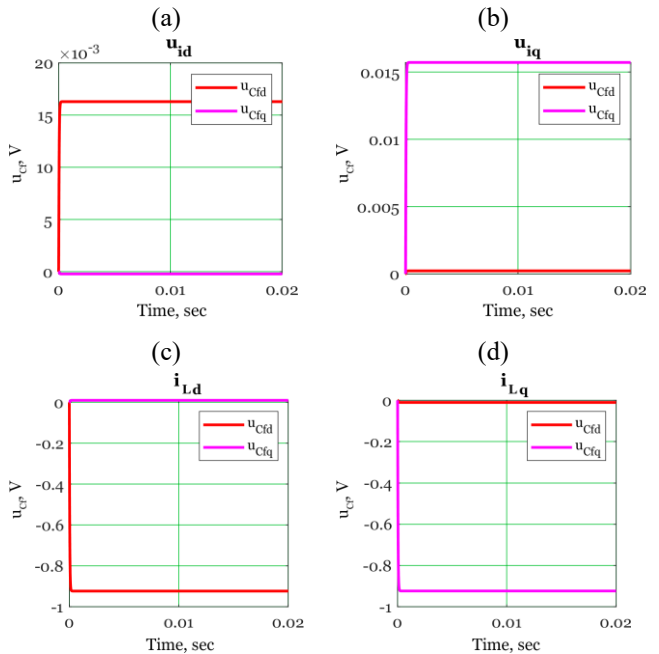


**Figure 11.** Transients in the closed-loop system with optimized linear-quadratic regulator (genetic algorithm parameters  $R_{mW_x} = 2$  and  $R_{mW_u} = 0.5$ ) during second model run: (a) channel “inverter voltage  $d$  – filter capacitor voltage”; (b) channel “inverter voltage  $q$  – filter capacitor voltage”; (c) channel “load current  $d$  – filter capacitor voltage”; (d) channel “load current  $q$  – filter capacitor voltage”

In this simulation, overshoot is completely absent for the following channels:  $u_{id} - u_{Cfd}$ ,  $u_{id} - u_{Cfq}$ ,  $u_{iq} - u_{Cfd}$ ,  $i_{Ld} - u_{Cfd}$ ,  $i_{Ld} - u_{Cfq}$  and  $i_{Lq} - u_{Cfd}$ . For the channel  $u_{iq} - u_{Cfq}$ , it tends toward zero and amounts to only 0.0058%. For channel  $i_{Lq} - u_{Cfq}$ , the overshoot is even more minor at 0.0008%, meaning

that overall it does not exceed the limits observed for most values in the previous simulation (Table 4).

The control system with the LQR regulator, employing weighting matrices of the form (28) and the state-feedback matrix (29), proves to be the best option among all the systems considered earlier. However, as previously noted, a steady-state error arises; therefore, in the final version of the ACS, a corrective element must be introduced to bring the system outputs along the  $d$  and  $q$  axes to the required levels.

The discrepancy in the results of the two simulations with identical GA settings can be attributed to the random nature of initial population generation. Nevertheless, it is also evident that in both cases the GA converges to the range where the OF attains its minimum values.

#### 4. Conclusions

In this work, based on the presence of time-stable voltage deviations from standardized values in the power supply systems of underground mines – deviations that exhibit nonlinear and stochastic characteristics – an adaptive control system for regulating the supply voltage of individual electrical consumers was developed. To implement the control process, the device operation is considered at a specific operating point, after which the obtained linear model is subjected to the linear-quadratic regulation method. At the same time, in the case of significant deviations from the operating point, the regulator parameters are retuned by an adaptive heuristic algorithm based on the evaluation of the actual characteristics of voltage deviations in both steady-state and dynamic modes.

In fact, the regulator is an optimization-type controller, and its parameters – the state and input weighting matrices – can be determined automatically. The operation of the linear-quadratic regulator was tested in a simulation format with randomly assigned weighting matrices. The results confirmed that it guarantees improved transient performance; however, the controller itself requires additional tuning.

The use of a genetic algorithm for optimizing the parameters of the linear-quadratic regulator is substantiated, as it enables the automated determination of its state and input weighting matrices. An analysis of the applicability of various objective functions in optimizing the dynamic voltage restorer controller confirmed the advisability of employing the integral absolute error, which is justified by the simplicity and generality of this indicator, as it accounts for both overshoot and transient response time.

The optimization of the state and input weighting matrices of the linear-quadratic regulator was performed using a genetic algorithm. An analysis was conducted to examine the influence of algorithm parameters, such as the mutation intensity of the controller parameters, on the quality of the evolutionary search. It was determined that a mutation intensity of 2 for the state matrix and 0.5 for the input matrix over 200 generations of the genetic algorithm ensures the best transient performance in the dynamic voltage restorer control channels, with a minimum integral absolute error value approaching 0.03 V. At the same time, overshoot is practically absent in all control channels, and the transient response time, when compared with the non-tuned system, is reduced by no less than 95%.

#### Author contributions

Conceptualization: OM, OS; Data curation: OM, MK; Formal analysis: IS, MK, VB, MB; Investigation: OM, IS, MK; Methodology: OM, IS; Project administration: OS, OM; Resources: OM, MK, VB, MB; Software: OM; Supervision: OS, OM; Validation: OM, IS, MK; Visualization: OM, MK; Writing – original draft: OM, OS; Writing – review & editing: OM, OS. All authors have read and agreed to the published version of the manuscript.

#### Funding

This research received no external funding.

#### Acknowledgements

We are sincerely grateful to the Kryvyi Rih National University administration for creating and maintaining favourable conditions for conducting research.

#### Conflicts of interest

The authors declare no conflict of interest.

#### Data availability statement

The original contributions presented in the study are included in the article, further inquiries can be directed to the corresponding author.

#### References

- [1] Kotiakova, M.G. (2023). *Aspects of development of modern management systems for improving the quality of electric energy in distribution networks of iron ore enterprises*. iScience.
- [2] Utegulov, B., Utegulov, A., Begentayev, M., Zhumazhanov, S., & Zhakipov, N. (2011). Method for determining parameters of isolation network voltage up to 1000 V in mining enterprises. *Proceedings of the IASTED International Conference on Power and Energy Systems and Applications Pesa 2011*, 50-53. <https://doi.org/10.2316/P.2011.756-028>
- [3] Utegulov, B., Utegulov, A., Begentayev, M., Zhakipov, N., & Sadvakasov, T. (2011). Method for determining the insulation in asymmetric networks with voltage up to 1000 V in mining enterprises. *Proceedings of the IASTED International Conference on Power and Energy Systems and Applications Pesa 2011*, 54-57. <https://doi.org/10.2316/P.2011.756-029>
- [4] DSTU EN 50160:2023. *Characteristics of voltage in public electricity supply networks* (EN 50160:2022, IDT). (2023). Retrieved from: [https://online.budstandart.com/ua/catalog/doc-page.html?id\\_doc=106226](https://online.budstandart.com/ua/catalog/doc-page.html?id_doc=106226)
- [5] Sinchuk, I.O. (2019). *Methodological principles for assessing the electrical efficiency of iron ore enterprises*. PP Shekerbatykh.
- [6] Shkrabets, F.P., & Pleshkov, P.G. (2010). *Fundamentals of power supply*. RVL KNTU.
- [7] Farhadi-Kangarlu, M., Babaei, E., & Blaabjerg, F. (2017). A comprehensive review of dynamic voltage restorers. *International Journal of Electrical Power & Energy Systems*, 92, 136-155. <https://doi.org/10.1016/j.ijepes.2017.04.013>
- [8] Moghassemi, A., & Padmanaban, S. (2020). Dynamic voltage restorer (DVR): A comprehensive review of topologies, power converters, control methods, and modified configurations. *Energies*, 13(16), 16. <https://doi.org/10.3390/en13164152>
- [9] Prasad, D., & Dhananjayulu, C. (2022). A review of control techniques and energy storage for inverter-based dynamic voltage restorer in grid-integrated renewable sources. *Mathematical Problems in Engineering*, 2022(1), 6389132. <https://doi.org/10.1155/2022/6389132>
- [10] Remya, V.K., Parthiban, P., Ansal, V., & Babu, B.C. (2018). Dynamic voltage restorer (DVR) – A review. *Journal of Green Engineering*, 8(4), 519-572. <https://doi.org/10.13052/jge1904-4720.844>
- [11] Madhusudan, R., & Ramamohan Rao, G. (2012). Modeling and simulation of a dynamic voltage restorer (DVR) for power quality problems-voltage sags and swells. *IEEE-International Conference on Advances in Engineering, Science and Management*, 442-447.

[12] Perera, K., Salomonsson, D., Atputharajah, A., & Alahakoon, S. (2006). Automated control technique for a single phase dynamic voltage restorer. *2006 International Conference on Information and Automation*, 63-68. <https://doi.org/10.1109/ICINFA.2006.374153>

[13] Bezzub, M., Bialobrzeski, O., & Todorov, O. (2023). Research on the distribution of harmonic power components in the power circuit of a dynamic voltage restorer. *Electrical Engineering and Power Engineering*, 1, 19-29. <https://doi.org/10.15588/1607-6761-2023-1-2>

[14] Purnawan, H., Mardlijah, & Purwanto, E.B. (2017). Design of linear quadratic regulator (LQR) control system for flight stability of LSU-05. *Journal of Physics: Conference Series*, 890(1), 012056. <https://doi.org/10.1088/1742-6596/890/1/012056>

[15] Setiawan, N., & Pratama, G.N.P. (2021). Application of LQR full-state feedback controller for rotational inverted pendulum. *Journal of Physics: Conference Series*, 2111(1), 012006. <https://doi.org/10.1088/1742-6596/2111/1/012006>

[16] Siostrzonek, T., Wójcik, J., Dutka, M., & Siostrzonek, W. (2024). Impact of power quality on the efficiency of the mining process. *Energies*, 17(22), 5675. <https://doi.org/10.3390/en17225675>

[17] Sir Elkhatem, A., & Naci Engin, S. (2022). Robust LQR and LQR-PI control strategies based on adaptive weighting matrix selection for a UAV position and attitude tracking control. *Alexandria Engineering Journal*, 61(8), 6275-6292. <https://doi.org/10.1016/j.aej.2021.11.057>

[18] Conte, G.Y.C., Marques, F.G., & Garcia, C. (2021). LQR and PID control design for a pneumatic diaphragm valve. *Proceedings of the 2021 IEEE International Conference on Automation/XXIV Congress of the Chilean Association of Automatic Control*, 1-7. <https://doi.org/10.1109/ICAACCA51523.2021.9465250>

[19] Vishal, & Ohri, J. (2014). GA tuned LQR and PID controller for aircraft pitch control. *Proceedings of the 2014 IEEE 6<sup>th</sup> India International Conference on Power Electronics*, 1-6. <https://doi.org/10.1109/IICPE.2014.7115839>

[20] Magaji, N., Hamza, M., & Dan-Isa, A. (2012). Comparison of GA and LQR tuning of static VAR compensator for damping oscillations. *International Journal of Advances in Engineering & Technology*, 2(1), 594-601.

[21] Marada, T., Matousek, R., & Zuth, D. (2017). Design of linear quadratic regulator (LQR) based on genetic algorithm for inverted pendulum. *MENDEL*, 23(1), 149-156. <https://doi.org/10.13164/mendel.2017.1.149>

[22] Abdullah, A.I., Mahmood, A., & Thanoon, M.A. (2023). Design of a linear quadratic regulator based on genetic model reference adaptive control. *Journal of Automation, Mobile Robotics and Intelligent Systems*, 16(3), 75-81. <https://doi.org/10.14313/jamris/3-2022/26>

[23] Ochoa-Giménez, M., Roldán-Peréz, J., García-Cerrada, A., & Zamora-Macho, J.L. (2015). Efficient multiple-reference-frame controller for harmonic suppression in custom power devices. *International Journal of Electrical Power & Energy Systems*, 69, 344-353. <https://doi.org/10.1016/j.ijepes.2015.01.013>

[24] Mykhailenko, O.Y., Sinchuk, I.O., Kotiakova, M.G., & Fedotov, V.O. (2025). Dynamic voltage restorer model for analysing the operational voltage stabilisation system at the underground mines' power grids. *Energy Saving, Energy, Energy Audit*, 4(207), 6-22. <https://doi.org/10.20998/2313-8890.2025.04.01>

[25] Hassanat, A., Almohammadi, K., Alkafaween, E., Abunawas, E., Hammouri, A., & Prasath, V.B.S. (2019). Choosing mutation and crossover ratios for genetic algorithms – A review with a new dynamic approach. *Information*, 10(12), 390. <https://doi.org/10.3390/info10120390>

[26] Immanuel, S.D., & Chakraborty, U.Kr. (2019). Genetic algorithm: An approach on optimization. *Proceedings of the 2019 International Conference on Communication and Electronics Systems*, 701-708. <https://doi.org/10.1109/ICCES45898.2019.9002372>

[27] Wright, A.H. (1991). Genetic algorithms for real parameter optimization. *Foundations of Genetic Algorithms*, 1, 205-218. <https://doi.org/10.1016/B978-0-08-050684-5.50016-1>

## Адаптивне керування напругою живлення електроприймачів підземних рудників

О. Сінчук, О. Михайленко, І. Сінчук, М. Котякова, В. Барановський, М. Барановська

**Мета** статті полягає у розробці автоматизованої системи стабілізації напруги живлення індивідуальних електроприймачів залізорудних шахт при її відхиленні від стандартизованих значень, що зумовлені непрогнозованими збуреннями у внутрішньорудниковоих системах електропостачання.

**Методика.** Для оперативної стабілізації напруги живлення шахтних електроприймачів використовувався динамічний відновлювач напруги. Базова система керування динамічним відновлювачем напруги розроблялася з використанням методів теорії керування, як-то лінійно-квадратичного регулювання. Для адаптації лінійно-квадратичного регулятора до дій непрогнозованих збурень застосовувалися методи евристичної оптимізації. У якості критерію прийнято інтегральну абсолютною похибку керування. Для перевірки якості переходів процесів при стабілізації напруги з використанням запропонованої системи застосовувався метод чисельного аналізу.

**Результати.** Розроблено адаптивну систему керування динамічним відновлювачем напруги для оперативної стабілізації напруги живлення індивідуальних електроприймачів залізорудних шахт. Визначено оптимальні параметри генетичного алгоритму, як-то, розмір популяції, інтенсивності мутацій вагових матриць стану і керування лінійного квадратичного регулятора, що забезпечують мінімальне значення інтегральної похибки керування, і, у наслідку, відсутність перерегулювання (наявні перерегулювання становили на більше 0.058%) та суттєве зменшення часу переходіного процесу (до 95%) порівняно з неоптимізованою системою.

**Наукова новизна.** Вперше запропоновано методику автоматизованого адаптивного налаштування лінійно-квадратичного регулятора динамічного відновлювача напруги для компенсації коливань напруги в електромережах підземних рудників з використанням генетичного алгоритму, який через використання інтегральної абсолютної похибки як універсального критерію якості регулювання при оптимальних параметрах еволюційного пошуку, дозволив забезпечити відсутність перерегулювання та скорочення часу переходіного процесу.

**Практична значимість.** Отримані результати можуть бути використані при розробці вбудованого програмного забезпечення для цифрових пристрійів керування динамічним відновлювачем напруги, що забезпечують компенсацію коливань напруги в режимі реального часу, підвищуючи якість електропостачання шахтних споживачів електроенергії.

**Ключові слова:** шахта, система електропостачання, керування напругою, динамічний відновлювач напруги, лінійно-квадратичний регулятор, генетичний алгоритм

## Publisher's note

All claims expressed in this manuscript are solely those of the authors and do not necessarily represent those of their affiliated organizations, or those of the publisher, the editors and the reviewers.